Symposium on Tornadoes
1976
Lubbock, TX

F. HISTORY OF SUCTION VORTICES

T. Theodore Fujita

The University of Chicago

1. INTRODUCTION

Who discovered the moon? The moon was there even before the first Homo Sapiens had settled on this planet Earth.

Ever since the early settlers in the Midwest discovered tornadoes, they must have seen small funnel-like clouds hanging around the main funnel. They could not, however, decide if they were separate tornadoes or some strange features of a single tornado.

Only about 100 tornadoes per year were confirmed by the U. S. Weather Bureau when the official collection of tornado data began in 1916. Obviously, the Weather Bureau did not count multiple funnel clouds as multiple tornadoes, thus ignoring them in compiling the annual tornado frequencies.

People, nonetheless, kept seeing the rather erratic damage left behind by tornadoes. They commented, for instance, "my house was badly damaged but the wind did not touch my neighbors..."

The Weather Bureau, in the early days, explained this strange act of tornadoes as being the touch down and skipping of the funnel cloud. One way or another, the general public accepted this explanation rather smoothly, saying the tornado lifted after damaging my house but before reaching the next-door neighbor....

Aerial photography during the 1950s unveiled the two-dimensional patterns of storm damage. Numerous photographs showed strange views in which houses were left standing surrounded by smashed structures. A text-book type tornado, acting alone, cannot possibly perform repeated touch downs and skippings to generate such a distribution of damage.

While flying in a Cessna over the paths of more than 150 tornadoes, large and small, intense and weak, Fujita and his collaborators took thousands of aerial photographs. These pictures, along with still and motion pictures, collected during the past two decades have led the author to come up with the idea of multiple-vortex tornadoes.

Namely, the wind field of a tornado is unlikely to be axially symmetric. The asymmetry is so significant that a tornado vortex is either accompanied by or broken up into several sub-tornado-scale vortices. The author termed these vortices the "suction vortices".

Other terms such as "secondary" and "satellite vortices" had been suggested, but they were rather misleading. After the passage of a tornado, severe damage and/or deaths occur predominantly inside the narrow bands marking the paths of these vortices. They represent the primary damage swaths with extremely high winds and pressure variations.

The term "satellite vortices" is also improper to use, because only about 60% of these vortices orbit around the tornado center, while others move differently.

2. DEFINITION OF SUCTION VORTICES (by Fujita and Forbes, as of July, 1976)

A suction vortex is a fast-spinning column of air embedded inside the tornado circulation, observable as a swirling dust cloud with or without a condensation funnel inside. The vertical acceleration of the air near the surface is greater than g, the gravitational acceleration, while the vortex diameter rarely exceeds 30 m (100 ft). The spinning rate of the vortex is estimated at 25 to more than 45 m/sec (100 mph). Its traveling speed, governed by the airflow inside the parent tornado, could be as fast as 90 m/sec (200 mph).

One or several suction vortices swirl concurrently within a tornado. The types and estimated occurrence probability of these vortices are shown in Table 1.

Table 1. Types of suction vortices to be found inside or in the vicinity of tornadoes. The probability denotes the estimated number of the suction swaths.

Types and Abbreviations	Prob.	Description and Ground Marks
Orbiting Vortex (OSV)	60%	Orbits around the tornado core (looping or scalloping mark)
Fringe Vortex (FSV)	20%	Spirals in toward the tornado core (crescent or spiral mark)
Central Vortex (CSV)	10%	Wobbles around near the tornado center (lineation mark)
Stray Vortex (SSV)	6%	Strays around outside the tornado core (lineation mark)
Instantaneous Vortex (ISV)	2%	Swirls momentarily (swirl mark or removal spot)
Peripheral Vortex (PSV)	2%	Develops some distance away from the parent funnel, often identified as a separate tornado

The internal circulation of suction vortices, often obscured by thick clouds of dust, is rarely seen by man. Their presence and the paths can be inferred by the ground marks such as removal or clearing bands, deposit lines, and high-wind swaths. Structures and objects along these swaths experience, in addition to the tornado's fury, abrupt pressure changes, coupled with horizontal gust, vertical suction, and twisting forces. Large missiles are likely to be generated by strong suction vortices.

The schematic location and movement of suction vortices is shown in Fig. 1. The number of orbiting vortices at a given time vary between 2 and 7 with an average number of 4. The central vortex, seen near the center of a small tornado, travels with the parent tornado while wobbling around its center.

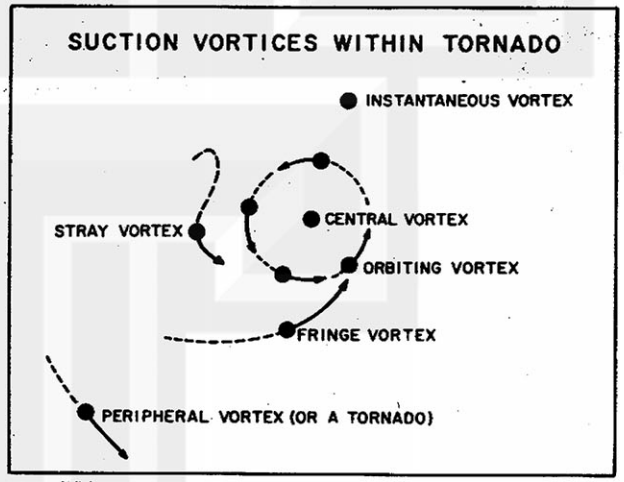

Fig. 1. Type of suction vortices within tornado. The orbiting vortices are the most popular ones. They circle around the tornado center but their life is short. Only a few vortices live long enough to complete one orbit.

3. NATURE OF SUCTION VORTICES

A suction vortex can schematically be divided into two parts, the inflow vortex and the helical vortex.

Inside the inflow vortex the air spirals up until it reaches the base of the helical vortex in which the air rises along helix trajectories (see Fig. 2).

If we assume an axial-symmetric, steady-state helical motion inside the helical vortex, the pressure gradient and

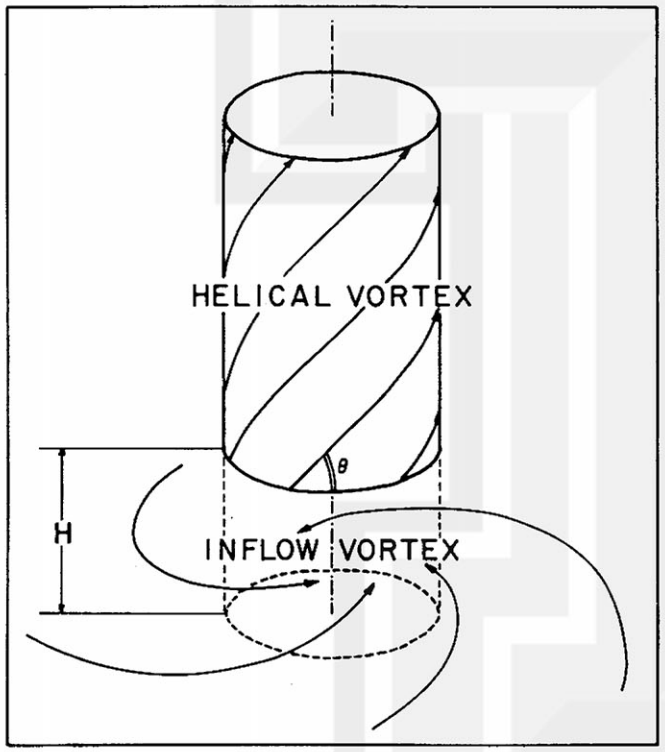

Fig. 2. A suction vortex consisting of two vortex parts. Inside the inflow vortex, the low-level air spirals in and rises, being accelerated by the vertical gradient of non-hydrostatic pressure. Upon entering the helical vortex, the air rises along helical paths.

the centrifugal force must balance, permitting us to equate

$$\frac{v_s^2 + w_s^2}{r_c} = \frac{1}{\rho}\frac{dP}{dr} \qquad (1)$$

where v_s and w_s are the tangential and vertical velocity of the air rising along a helix; r_c, the radius of curvature of the helix; ρ, the air density; and dP/dr, the pressure gradient. By expressing the ascending angle of the helix by θ, we write

$$w_s = v_s \tan\theta$$

$$r_c = r \sec^2\theta \qquad (2)$$

The above equations permit us to reduce Eq. (1) into

$$\frac{v_s^2 \ (1 + \tan^2\theta)}{r \sec^2\theta} = \frac{1}{\rho}\frac{dP}{dr}$$

or

$$\frac{v_s^2}{r} = \frac{1}{\rho}\frac{dP}{dr}$$

This is no more than the cyclostrophic wind equation. We are, thus, able to compute the pressure distribution inside the helical vortex as a function of v_s, the tangential component only. The vertical velocity, w_s, does not contribute to the pressure distribution.

The standard method of pressure integration, under the Rankine vortex assumption, permits us to express the deficit pressure by

$$P_\infty - P_r = \frac{1}{2}\rho V_s^2\left(\frac{R_s}{r}\right)^2 \quad \text{outside the core} \qquad (4)$$

$$P_\infty - P_r = \rho V_s^2 - \frac{1}{2}\rho V_s^2\left(\frac{r}{R_s}\right)^2 \quad \text{inside the core} \qquad (5)$$

where P_∞ is the environmental pressure; P_r, the pressure at the distance r; and R_s, the radius of maximum wind.

Although the deficit pressure is constant along the vertical inside a helical vortex, it decreases as the height inside the inflow vortex decreases.

If we express the deficit pressures at the top of the inflow vortex and at the surface by ΔP_H and ΔP_0, respectively, we may write

$$\Delta P_0 = (1 - f)\Delta P_H \qquad (6)$$

where f denotes the filling factor. When $f = 1.00$ or 100% filling, no pressure gradient exists on the surface where $u = v = w = 0$. In reality, however, f is smaller than 1.00 resulting in a fractional filling such as 50%, 25% filling, etc.

The mean vertical acceleration inside the inflow vortex can be expressed by

$$\bar{a} = \frac{1}{\rho}\frac{(P_0 - \Delta P_0) - (P_H - \Delta P_H)}{H} - g$$

$$= \frac{1}{\rho}\frac{\rho g H + (\Delta P_H - \Delta P_0)}{H} - g$$

$$= \frac{1}{\rho}\frac{\Delta P_H - \Delta P_0}{H}$$

$$= \frac{f}{\rho}\frac{\Delta P_H}{H} \qquad (7)$$

The maximum acceleration occurs at the center of the vortex where the deficit pressure is largest. Combining Eq. (7) with Eq. (5) at $r = 0$, we obtain the vertical acceleration at the center of the inflow vortex.

$$\bar{a}_{(CENTER)} = f\frac{V_s^2}{H} \qquad (8)$$

Naturally, the vertical acceleration is the largest when $f = 1$. (Table 2)

Table 2. Vertical acceleration acting upon the air at the center of the inflow vortex (in g unit).

Inflow Depth meters(ft)	Maximum tangential velocity in m/s(mph) 10(22)	20(45)	30(67)	40(89)	50(112)
5(16)	2xg	8xg	18xg	33xg	51xg
10(33)	1	4	9	16	26
15(49)	0.7	3	6	11	17
20(66)	0.5	2	5	8	13
25(82)	0.4	2	4	7	10
30(98)	0.3	1	3	5	9

The vertical acceleration which drives convection currents in meteorology is the buoyancy force.

$$a = g\frac{T' - T}{T} \qquad (9)$$

which is only a small fraction of g, the gravitational acceleration. The vertical acceleration in Eq. (8) is induced by the vertical gradient of the non-hydrostatic pressure, which is about two orders of magnitude larger than the buoyancy acceleration.

The helical vortex literally sucks up the air spiraling inside the inflow vortex. "Suction vortex" would be the most suitable term in expressing the nature and behavior of such a vortex.

4. HISTORICAL ASPECTS OF SUCTION VORTICES

After the wake of the Scottsbluff tornado of June 27, 1955, Van Tassel (1955) found CIRCULAR MARKS in aerial pictures (see Fig. 3).

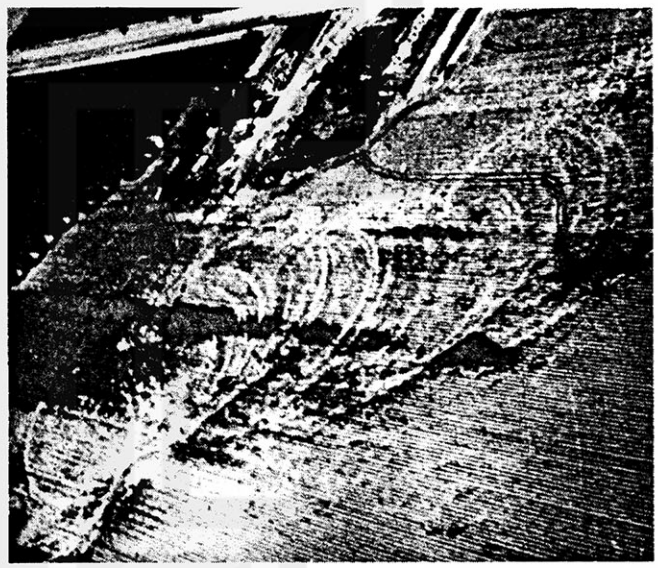

Fig. 3. Circular marks left by the Scottsbluff tornado of June 27, 1955. After Van Tassel (1955).

Under the assumption that the marks were left by a SINGLE OBJECT caught in the tornado funnel, the rotational speed of the object was computed to be 484 mph.

This speed is apparently too high because the assumption of multiple objects will cut down the rotational speed to $484 \div n$.

Prosser's (1964) SURFACE MARKS near Shelby, Iowa on May 5, 1964 define the axis of most intense destruction. They gave the impression that an enormous vacuum cleaner had swept the ground clean of vegetation, loose soil, and other movable objects.

Fujita (1966) photographed, from 1000 ft, the CYCLOIDAL MARKS left by the Kokomo tornado of April 11, 1965. He found that the reflectivity of the marks change considerably according to the viewing angle relative to the sun.

The Barrington, Illinois tornado of April 21, 1967 was surveyed both from the air and the ground. The light marks in the field consisted of short pieces of corn stubble deposited on a plowed field. Fujita, Bradbury, and Black (1967) measured the deposit as 8" high and 5' wide. The marks gave the impression of a deposit or litter left by the suction forces of the tornado (see Fig. 4). They called the marks CYCLOIDAL SUCTION MARKS.

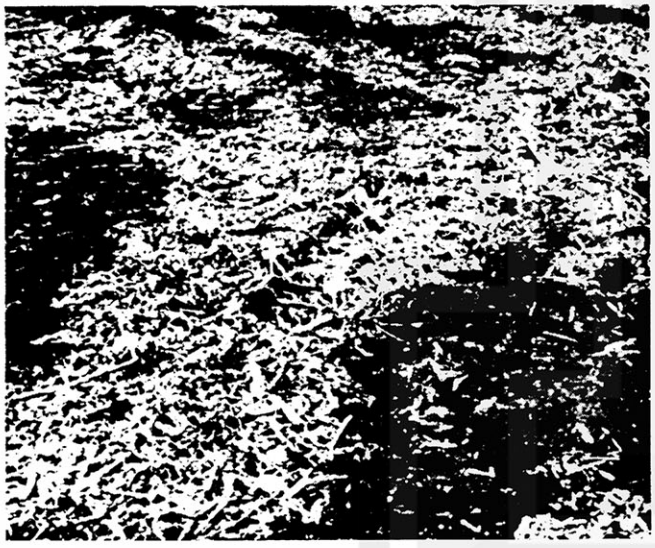

Fig. 4. A close-up view of a cycloidal mark in the wake of the Barrington tornado of April 21, 1965. Photo by Fujita standing on a 6-ft ladder.

Waite and Lamoureux (1969) obtained a 458-mph speed using the Charles City, Ia. tornado of March 15, 1968 and Van Tassel's hypothesis. The speed, thus computed, will have to be divided by n, the number of items which circled around the tornado's core. The term CORN STRIATION was used in identifying the ground marks.

In their comprehensive study of the Palm Sunday Tornadoes of April 11, 1965, Fujita, Bradbury, and Van Thullenar (1970) hypothesized that the ground marks represented the paths of the SUCTION SPOTS. 4 to 5 suction spots were confirmed as having circled simultaneously around their parent tornado core. It was assumed that the suction effects were concentrated at several spots at the radius of maximum wind. The traveling speed of the spots were 104 to 118 mph.

While making an aerial survey of the Lubbock, Texas tornado of May 11, 1970, Fujita (1970) noticed the circular bands of heavy damage across the city (refer to Fig. 5, drawn in the helicopter). He postulated that the circular bands called SUCTION SWATHS represent the paths of suction spots. 26 of the 28 deaths in the city occurred within the suction swaths.

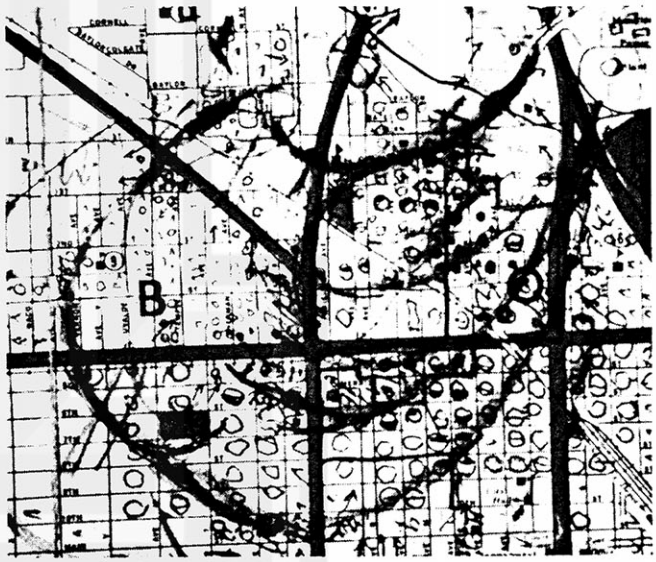

Fig. 5. Original sketch of the suction swaths across Lubbock, drawn by Fujita in a low-flying helicopter.

Ward (1970) succeeded in producing TWIN AND MULTIPLE VORTICES in his laboratory model at NSSL. These vortices circled around the core of his laboratory tornado.

On April 30, 1971, Fujita (1971) made aerial photographs of a giant dust devil with multiple vortices circling around its center. As shown in Fig. 6 these vortices intensified at the core boundary where the largest convergence is expected to occur. Not all vortices made one complete rotation around the core, indicating that their life is very short.

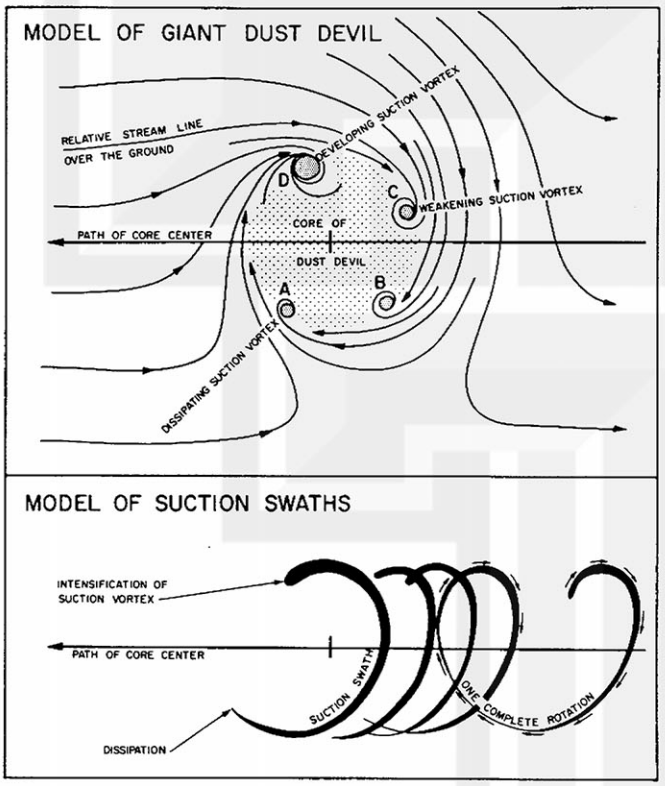

Fig. 6. A model of a giant dust devil accompanied by several subvortices. These subvortices formed inside the sector where the convergence of the inflow air was most significant.

The Japanese tornado of July 7, 1971 showed definite evidence of the suction spots in rotation. One of the six suction swaths found in the north suburb of Tokyo moved across a sweet potato field. The final direction of the stretched vines gave the patterns of the fossil winds which are highly rotational and convergent. Fujita et al (1972) called these vortices the SUCTION VORTICES inside the tornado.

Suction vortices were known to rotate around the tornado center. The

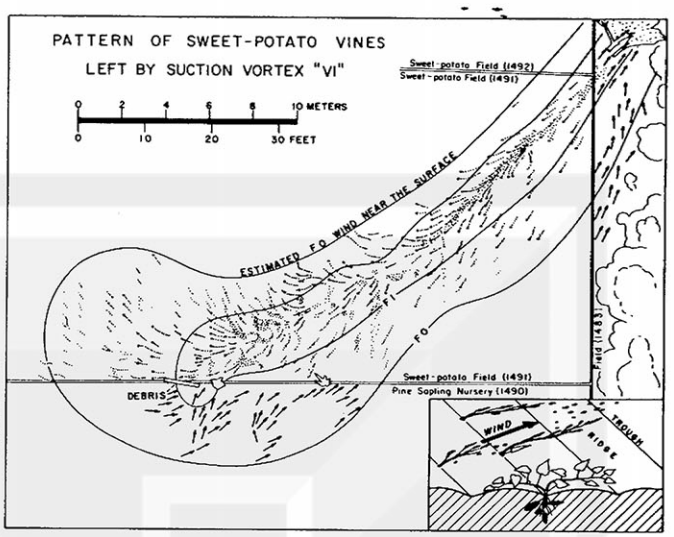

Fig. 7. Fossiled streamlines of the final wind preserved by the stretched vines in a sweet potato field. The July 7, 1971 tornado near Tokyo left behind damage patterns very similar to those of U. S. tornadoes.

Iowa tornado of September 28, 1972 did something different. The NWS at Dubuque, Ia. called the author to determine if there were 26 tornadoes or not. The author's aerial survey revealed the paths of numerous suction vortices. The swath of a STRAY SUCTION VORTEX (SSV) and an INSTANTANEOUS SUCTION VORTEX (ISV) were identified (see Figs. 8 and 9).

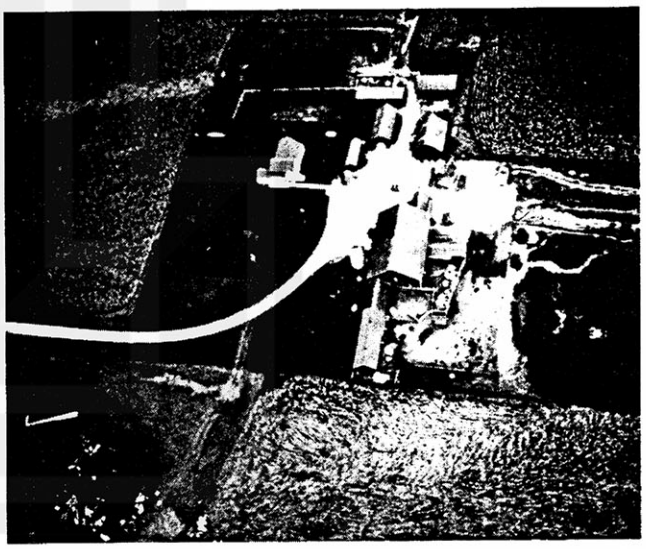

Fig. 8. Two stray vortices which moved along two parallel tracks on both sides of an Iowa farm. Even weak outbuildings were intact in the cattle feed area. The Sept. 28, 1972 tornado was accompanied by different types of suction vortices.

Fig. 9. Fossiled streamlines of an instantaneous suction vortex in a corn field left by the Sept. 28, 1972 tornado. Apparently, the vortex swirled momentarily and disappeared.

The Pearsall, Texas tornado of April 15, 1973, surveyed by Fujita (1973), moved across a young wheat field, leaving behind a number of suction swaths. Stalks were blown down and pulled into the center of the suction vortex, resulting in a swirling pattern of wheat stalks (see Fig. 10). The suction swaths are made visible by the differential reflection of the sunlight. As a result, the swaths are visible only from certain directions relative to the sun. This is why suction swaths had not been photographed in the past (see Figs. 11-14).

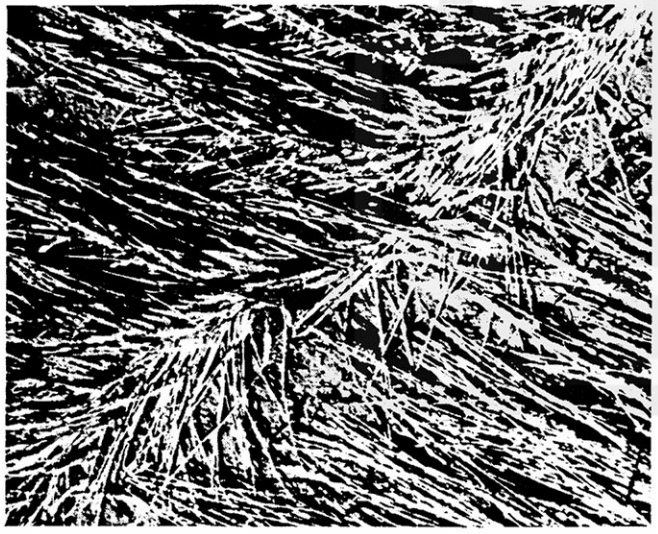

Fig. 10. A swirling pattern of wheat stalks along the path of a suction vortex.

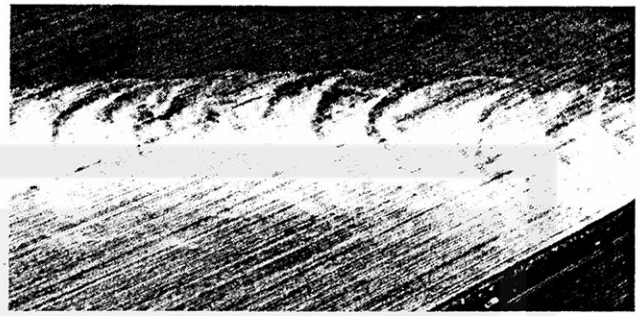

Fig. 11. The appearance of vortex swaths vary according to the viewing direction. This picture was taken while looking toward the north. Swaths are very distinct. Pearsall tornado of April 15, 1973.

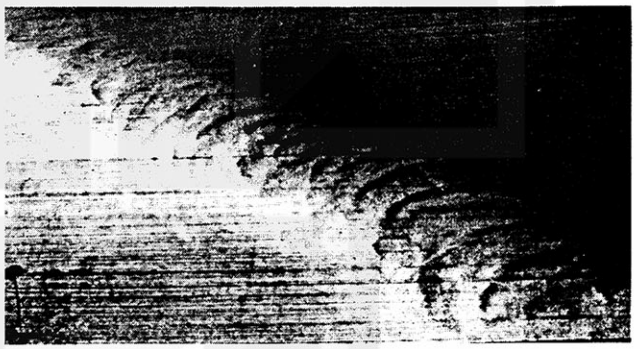

Fig. 12. A view looking toward the northwest.

Fig. 13. A view looking toward the northeast.

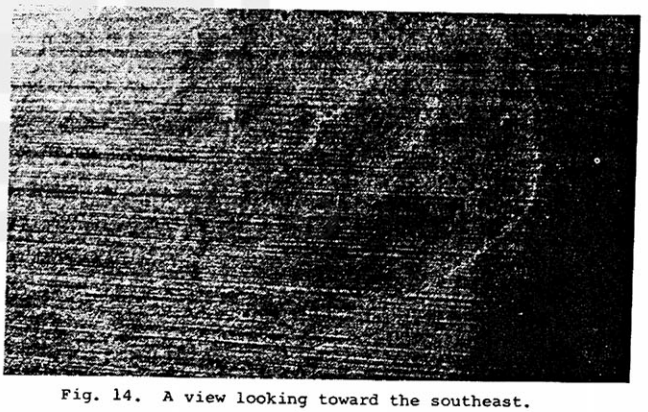

Fig. 14. A view looking toward the southeast.

The superoutbreak of 148 tornadoes on April 3-4, 1974 left behind a number of paths showing the activities of suction vortices. Shown in Figs. 15-17 are the typical dimensions of the tornado core, made visible by the paths of a central suction vortex, orbiting suction vortices, and twin suction vortices of a giant core tornado. The figures were chosen from 3000 aerial photos taken after the outbreak.

Fig. 15. The path of a small tornado on April 3, 1974 near Resaca, Georgia.

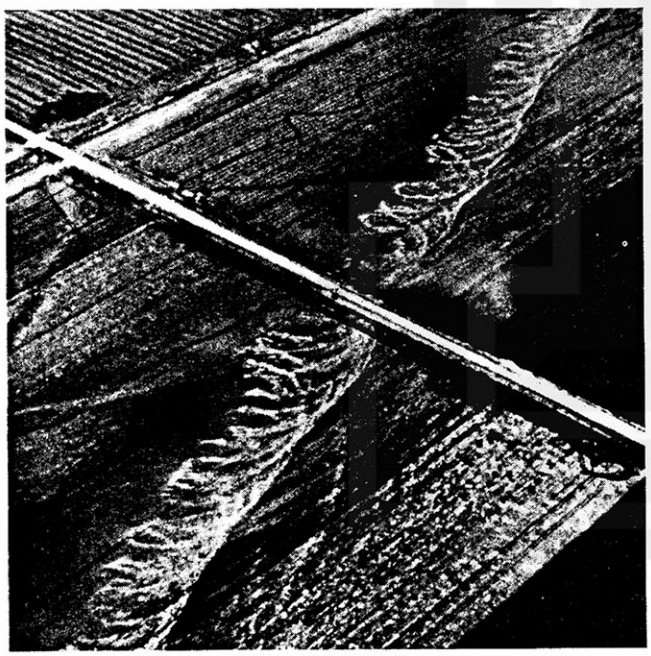

Fig. 16. The looping marks of a medium diameter tornado on April 3, 1974 near Anchor, Ill.

Fig. 17. Giant-sized looping marks on April 3, 1974 near Homer Lake, Illinois. Occasional double lines suggest that a suction vortex within a giant tornado splits into twin vortices.

Numerous funnel pictures also were collected from the public in the storm areas. of interest are the rapid changes of suction vortices made visible by condensation funnels inside. A sequence of Xenia tornado pictures by Mr. Hess shows a rapid change of suction vortices (see Figs. 18 and 19).

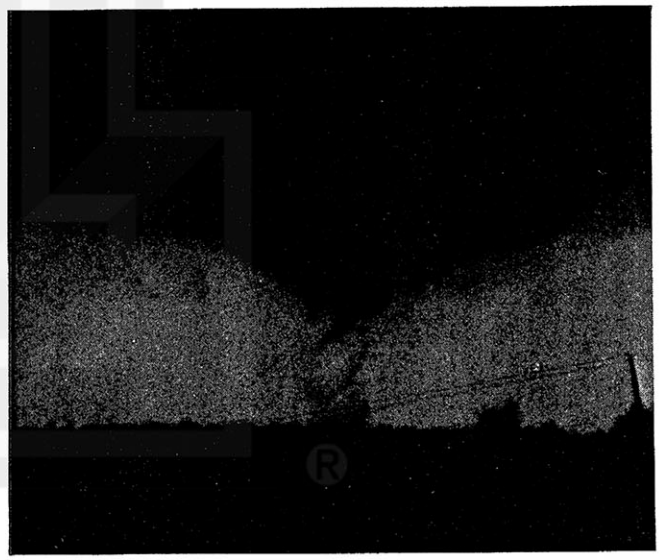

Fig. 18. The early stage of the Xenia tornado of April 3, 1974 showing helix-shaped condensation funnels (Photo by Mr. Hess).

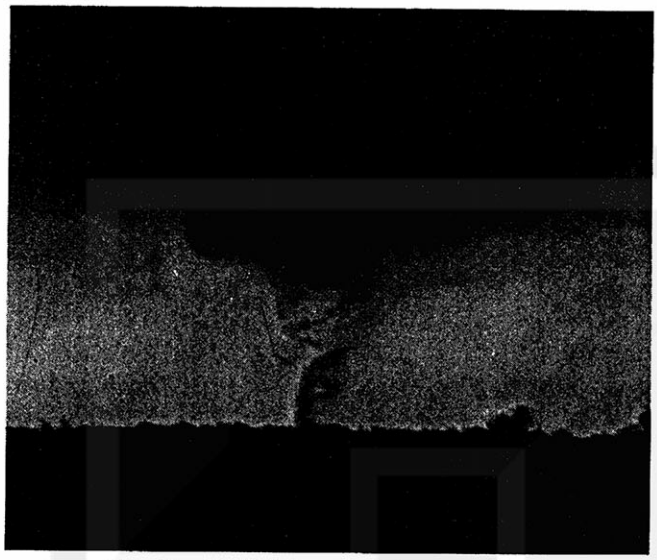

Fig. 19. Several seconds later a small, violent suction vortex formed near the ground and rose rapidly (Photo by Mr. Hess).

The appearance of looping marks in an open field implies the paths of non-violent vortices, because they are characterized by narrow bands of the deposit. The suction vortices, apparently, failed to lift the light objects; they were left behind. The situation is entirely different, once the looping paths are traced into the forest. Trees were snapped, blown down, or uprooted along the looping paths, revealing that the suction vortices were violent at the level of the tree tops in the forest (see Fig. 20).

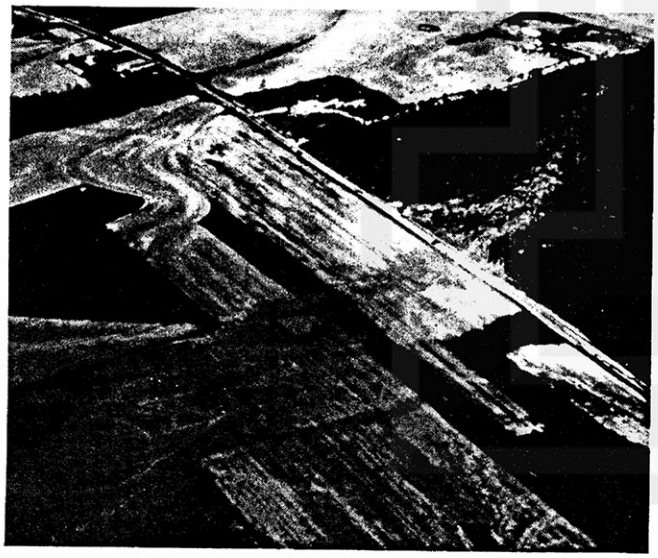

Fig. 20. Paths of the orbiting vortices (OSV) inside the Second Tanner tornado of April 3, 1974. The looping marks, characterized by deposit lines in the open field, turned into the bands of blown-down trees in the forest.

On the day of the Omaha tornado, May 6, 1975, a violent tornado wiped out Magnet, a small Nebraska community. One of the best looping marks was photographed from 500 ft above an open field (see Fig. 21).

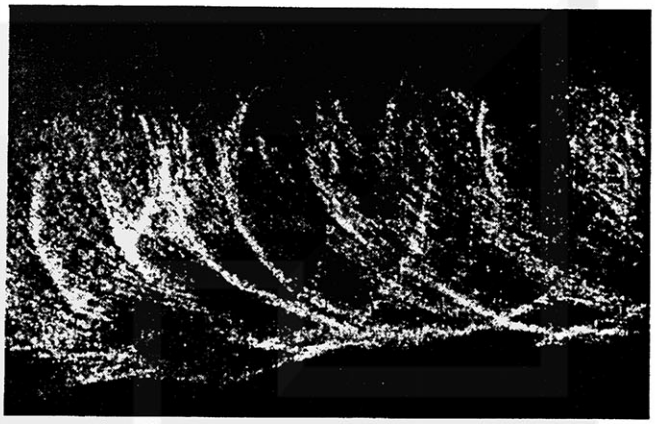

Fig. 21. Looping marks left by the Magnet tornado of May 6, 1975.

The Sadorus tornado of March 20, 1976 was filmed from two opposite directions Without knowing of the existence of these movies, Fujita and Forbes made an aerial photographic survey on the 21st. There were dark looping marks with 150 to 160 meter widths. The diameter of the swirling dust column, as shown in Fig. 22, was 350 meters.

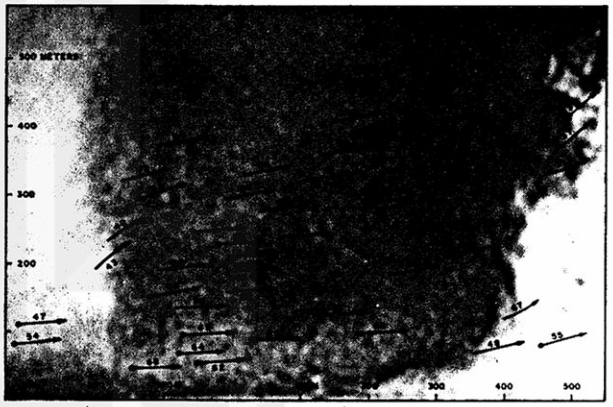

Fig. 22. Dust column of the Sadorus tornado of March 20, 1976. The maximum speed of the column at 200m above the ground was 202 mph. This, however, does not represent the maximum wind speed hidden deep inside the column. Refer to Fujita, Forbes, and Umenhofer (1976).

This evidence is very important because the edge of the dust column was located at a radius--which was about twice the radius of the core--where the maximum winds are expected. Figure 22, thus, leads to an interpretation as follows:

Total horizontal speed at h = 100 m, r = 180 m	69 m/sec
Traveling speed of tornado	20 m/sec
Tangential speed at h = 100 m, r = 180 m	49 m/sec
Rankine tangential speed at r = 80 m core radius	110 m/sec
Total horizontal speed at h = 100 m, r = 80 m	130 m/sec 290 mph*

*This speed includes partial tangential speed of OSVs hidden inside. By adding 25 to 30 mph, the maximum wind speed at h = 100 meters is estimated to be 315 to 320 mph.

The total horizontal speed at h = 40 m was 62 - 65 m/sec, indicating, naturally, a decrease of the maximum wind speed toward the ground.

The looping marks, on the other hand, show that the R/T ratio (Revolving speed/Translational speed) of orbiting vortices was 2.5. Another independent estimate of the maximum wind speed based on these ground marks is

Traveling speed of tornado	20 m/sec
Revolving speed of OSVs	50 m/sec
Max. traveling speed of OSVs	70 m/sec
or about	155 mph**

**This speed does not include the tangential speed of OSV. By adding 50 to 100 mph, the max, wind speed is estimated to be 205 to 255 mph.

The mean values of the estimated wind speeds are

from movie	317 mph
from ground marks	230 mph
difference	87 mph

The error is significant, probably because we still do not know the structure of tornadoes including their subvortices.

This result boils down to a speculative conclusion: that the photogrammetric computations and interpretations currently available are still inaccurate. Needed in estimating the maximum wind speeds of tornadoes are the detailed analyses of a number of violent tornadoes based on movies and aerial photographs together.

When a suction vortex travels over a city its kinetic energy at the lowest levels will be lost, thus reducing the street-level wind significantly. As soon as the vortex moves out of the city, however, its energy is restored.

The Lafayette tornado of March 20, 1976 showed a remarkable recovery of orbiting vortices after their travel across a forest and several houses. Trees were uprooted and houses were smashed to the ground, leaving a band of debris strewn over 200 m into the field. Aerial photographs of the forest and the houses showed no signs of suction vortices which might have existed above tree-top and roof-top levels.

Fig. 23. Looping marks which redeveloped in an open field to the northeast of the two houses destroyed by the Lafayette tornado of March 20, 1976.

Less than 50 m downwind in the open field, however, several looping marks formed and continued further, implying that a number of orbiting vortices had moved over these trees and houses.

During the past 22 years, since Van Tassel attempted to determine the tornado wind speed based on a single object assumption, our knowledge of the sub-tornado-scale vortices has been increasing rather steadily. Accelerated data gathering, which has been very successful in recent years, has contributed a lot in confirming the existence of suction vortices within large core tornadoes.

It is expected that the role of suction vortices in missile generation and localized damage mechanisms will be investigated in the coming years. In the meantime, however, it is necessary that the data collection system dealing with violent tornadoes be expanded on a nationwide scale.

REFERENCES

Fujita, T. T., 1966: Aerial Survey of the Palm Sunday Tornadoes of April 11, 1965. SMRP Res. Paper 49, Univ. of Chicago, 35 pp.

Fujita, T. T., D. L. Bradbury, and P. G. Black, 1967: Estimation of tornado wind speeds from characteristic ground marks, SMRP Res. Paper 69, Univ. of Chicago, 19 pp.

Fujita, T. T., 1970: The Lubbock Tornadoes: A Study of Suction Spots. Weatherwise, 23, 160-173.

Fujita, T. T., D. L. Bradbury, and C. F. Van Thullenar, 1970: Palm Sunday Tornadoes of April 11, 1965. Mon. Wea. Rev., 98, 29-69.

Fujita, T. T., 1971: Proposed Mechanism of Suction Spots accompanied by Tornadoes. Preprint of the 7th Conf. on Severe Local Storms, 208-213.

Fujita, T. T., K. Watanabe, K. Tsuchiya, and M. Shimada, 1972: Typhoon-associated tornadoes in Japan and New evidence of suction vortices in a tornado near Tokyo, J. of Met. Soc. of Japan, 50, 431-453.

Fujita, T. T., 1973: FPP Classification of all tornadoes. Letter to NWS Offices dated May 10, 1973. 15 pp.

Fujita, T. T., G. S. Forbes, and T. A. Umenhofer, 1976: Close-up View of 20 March 1976 Tornadoes: Sinking Cloud Tops to Suction Vortices. Weatherwise, 29, 116-131.

Prosser, N. E., 1964: Aerial photographs of a tornado path in Nebraska, May 5, 1964. Mon. Wea. Rev., 92, 593-598.

Van Tassel, E. L., 1955: The North Platte Valley Tornado Outbreak of June 27, 1955. Mon. Wea. Rev., 83, 255-264.

Waite, P. J. and C. E. Lamoureux, 1969: Corn Striations in the Charles City Tornado in Iowa. Weatherwise, 22, 55-59.

Ward, N. B., 1970: The Exploration of certain features of tornado dynamics using a laboratory model. NOAA Tech. Memo ERLTM-NSSL 52, 22 pp.

Acknowledgements:

The research work on Sections 1, 3, 4, 5, and 6 of this summary paper has been sponsored by NRC under Contract AT(49-24)-0239 and NOAA under Grant 04-4-158-1.

PHOTOGRAMMETRIC ANALYSES OF TORNADOES

T. Theodore Fujita, et al.

The University of Chicago

A. INTRODUCTION AND SUMMARY

Since the Dallas tornado of April 2, 1957, was analyzed photogrammetrically by Hoecker, analyses of movies have become a promising means of determining wind speeds of tornadoes. The so-called "photogrammetric analysis" has become so popular that a number of researchers have accomplished object tracking and subsequent computations.

Dr. Golden, the previous speaker, summarized the estimated tornado wind speeds tabulated in his paper. For further examination of the photogrammetric methodology, results of movie analyses were extracted from Golden's paper.

This table reveals that the photogrammetric analyses, currently performed by various researchers, are not always as reliable as the users think they are. The Parker tornado of April 3, 1974, for example, was analyzed by at least three researchers. During the Conference on April 3-4, 1974 Tornadoes, held at the University of Chicago on July 10, 1974, Fujita presented in his movie the

Translational velocity of tornado	50 mph
Revolving velocity of Suction Vortex around Parent Tornado	90 mph
Tangential (spinning) velocity of Suction Vortex	80 mph
Total windspeed ...	220 mph

Wind speed	Tornado	References in Golden's paper
170[a] mph	Dallas, 1957	Hoecker (1960)
112[a]	Fargo, 1957	Fujita (1960)
130	Kankakee, 1963	Goldman (1965)
144	Waterspout, 1967	Golden (----)
126	Kona, 1971	Zipser (1976)
176	Union City, 1973	Golden and Davies-Jones (1975)
155	Salina, 1973	Zipser (----)
220[b]	Parker, 1974	Fujita (1974)
170[b]	Parker, 1974	Agee (1975)
222[b]	Parker, 1974	Forbes (in this paper)
284[s]	Parker, 1974	Forbes (in this paper)
200[b]	Xenia, 1974	Fujita (1975)
265[s]	Xenia, 1974	Fujita (1975)
220	Xenia, 1974	Golden and Purcell (----)
159	Oshkosh, 1974	Bleçhman (1975)
170[b]	Great Bend, 1974	Golden and Purcell (1975)
202[b]	Sadorus, 1976	Umenhofer and Fujita (in this paper)

[a]add translational speed, 20 to 30 mph; [b]does not include tangential velocity of suction vortex; [s]suction vortex included.